Available online at www.sciencedirect.com
ScienceDirect
Journal of Hazardous Materials 153 (2008) 269–275
Journal of Hazardous Materials
www.elsevier.com/locate/jhazmat

Optimizing the operating parameters of corona electrostatic separation for recycling waste scraped printed circuit boards by computer simulation of electric field

Jia Li, Hongzhou Lu, Shushu Liu, Zhenming Xu *

School of Environmental Science and Engineering, Shanghai Jiao Tong University, 800 Dongchuan Road, Shanghai 200240, People's Republic of China

Received 20 May 2007; received in revised form 18 August 2007; accepted 20 August 2007
Available online 22 August 2007

Abstract

The printed circuit board (PCB) has a metal content of nearly 28% metal, including an abundance of nonferrous metals such as copper, lead, and tin. The purity of precious metals in PCBs is more than 10 times that of rich-content minerals. Therefore, the recycling of PCBs is an important subject, not only from the viewpoint of waste treatment, but also with respect to the recovery of valuable materials. Compared with traditional process the corona electrostatic separation (CES) had no waste water or gas during the process and it had high productivity with a low-energy cost. In this paper, the roll-type corona electrostatic separator was used to separate metals and nonmetals from scraped waste PCBs. The software MATLAB was used to simulate the distribution of electric field in separating space. It was found that, the variations of parameters of electrodes and applied voltages directly influenced the distribution of electric field. Through the correlation of simulated and experimental results, the good separation results were got under the optimized operating parameter: $U = 20$–30 kV, $L = L_1 = L_2 = 0.21$ m, $R_1 = 0.114$, $R_2 = 0.019$ m, $\theta_1 = 20^\circ$ and $\theta_2 = 60^\circ$.

Keywords: Printed circuit boards; Electric field; Computer simulation; Corona electrostatic separation

1. Introduction

The production of printed circuit boards (PCB) is the basis of the electronic industry as it is the essential part of almost all electrical and electronic equipments (EEE). New technological innovation continues to accelerate the replacement of equipment leading to a significant increase of waste PCBs that includes a new environmental challenge. In normal PCBs, plenty of toxic materials including heavy metal, PVC plastic and brominated flame retardants can be easily found. However, just like the two-sided coin, the scrap PCBs contain many kinds of metals, which are a rich mine of wealth. The PCBs contain nearly 28% metals [1] which have abundant nonferrous metals such as Cu, Pb, Sn, etc. [2], and the purity of precious metals which is about more than 10 times of rich-content mineral. Therefore, recycling of PCB is an important subject not only from the treatment of waste but also from the recovery of valuable materials.

The hydrometallurgy and pyrometallurgical method for treating waste PCBs could generate heavy environmental pollution [3–5]. Because the mechanical method was easy to industrialization and without secondary pollution, it was the most promising method to recycling resources from waste PCBs. The mechanical process was: (1) the waste PCBs were scraped to the mixture of particles of metals and nonmetals by crushers; (2) separated the mixture with the separator. The key of the process was separation. The metals were completely stripped from nonmetal base plates when the waste PCBs were scraped to the small particles with the size below 0.6 mm [6]. The corona electrostatic separation (CES) was the effective method for separating small particles at this size range. The CES had no wastewater or gas during the process and it had high productivity with a low-energy cost, as shown in Table 1. The structural representation of laboratory corona electrostatic separator was shown in Fig. 1. The electric vibratory feeder ensures a monolayer of granular material on the surface of the rotating roll. The high-voltage electrostatic field is generated by corona electrode and electrostatic electrode. Metal and nonmetal particles entering this field is mainly subjected to electrostatic induction and "ion

* Corresponding author. Tel.: +86 21 54747495; fax: +86 21 54747495.
E-mail addresses: zmxu@sjtu.edu.cn, okokjiajia@hotmail.com (Z. Xu).

0304-3894/$ – see front matter © 2007 Elsevier B.V. All rights reserved.
doi:10.1016/j.jhazmat.2007.08.047

Table 1
Comparison of three kinds of PCBs mechanical treatment methods

Process	Environment implication	Power (kW)	Productivity (t/h)
Air-current separation	Releasing dust	4	0.1–0.5
Fluid bed separation	Causing waste water including toxic heavy metals	1.1	0.5–0.8
Corona electrostatic separation	None	0.2	0.5–1.0

Source: http://www.machinery.com.cn.

bombardment" (corona charge), respectively. The metal particles discharge rapidly to the earthed electrode, while the charged nonmetal particles are "pinned" by the electric image force to the rotating roll, and move with it, finally fall in the hold tanks. The electric field forces act differently on the two kind of particles, which achieves the separation goal.

The differences of forces exerting on the materials caused different trajectories of particles. The electric field was one of main factors which affected the forces. The strength of electric field was decided by the operating parameters of electric poles and applied voltage. Because the characteristic of waste PCB scraps is different from the minerals, during the separation the operating parameters of separators are more complex. Consequently, the computer simulation method is a vital tool for the research and development of recycling process of CES. And there was no study about using computer simulation to optimize the operating parameters of CES in recycling waste PCBs. So, the numerical simulating software MATLAB was used to optimize the separating efficiency of corona electrostatic separator in this paper. The distributions of electric field of CES were simulated by MATLAB. The influence of operating parameters to the distributions of electric field and separating results were theoretically analyzed. A series experiments were used to verify the theoretical analyze results. On the basis of theoretical analyze and experimental results, the operating parameters of positions of electric electrodes and applied voltage were defined, which offered the theoretical basis for separating metals and nonmetals from waste PCBs by CES.

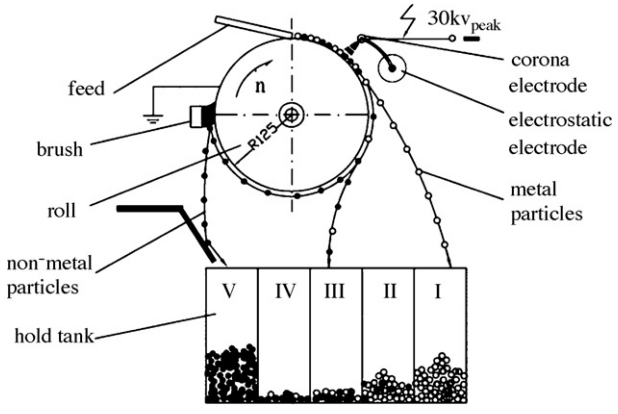

Fig. 1. The structural representational of laboratory roll-type corona electrostatic separator.

2. Methodology

The software of MATLAB is a high-level technical computing language and interactive environment for algorithm development, data visualization, data analysis, and numerical computation. The partial differential equation (PDE) tool box was a convenient and fast tool to simulate electrostatic field in CES which provides a powerful and flexible environment for the study and solution of partial differential equations in two space dimensions and time in MATLAB 7.0. According to different geometric models and boundary conditions, corresponding electric potential and electric-field strength distributions were plotted as a two or three dimension diagram. Because the lengths of electric poles were much bigger than their diameters, we considered the electrostatic field had no variation along the axial direction. The electrostatic field could be treated as a two-dimension problem. Fig. 2 shows the geometric model used in electrostatic field simulation.

In order to simulate the electric field it is assumed that: (1) the influence of space charges to electric field was neglected; (2) the particles' self electric fields were neglected; (3) the interactivity of particles was neglected. In the process of simulation, the radius of rotating roll was 0.114 m and the radius of corona wire was 0.3 mm. The difference between two adjacent electric field lines was set to 5000 V/m.

2.1. Constructions of electrodes

As shown in Fig. 3(a and b), the lines of electric field strength between electrodes in CES were plotted by PDE tools in MATLAB. In Fig. 3(c), the vertical axis indicated the electric field strength on the surface of rotating roll; the horizontal axis indicated the included angles of horizontal line and link of center of rotating roll and the point. In Fig. 3(a), the electric field strength on the surface of rotating roll was Gaussian distribution and the maximum value was at the link of center of rotating roll and corona electrode. In Fig. 3(b), the construction of composite

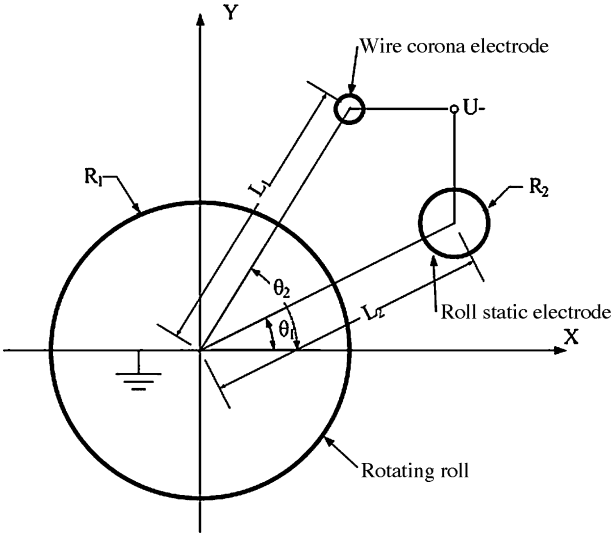

Fig. 2. The geometric model used in electrostatic field simulation.

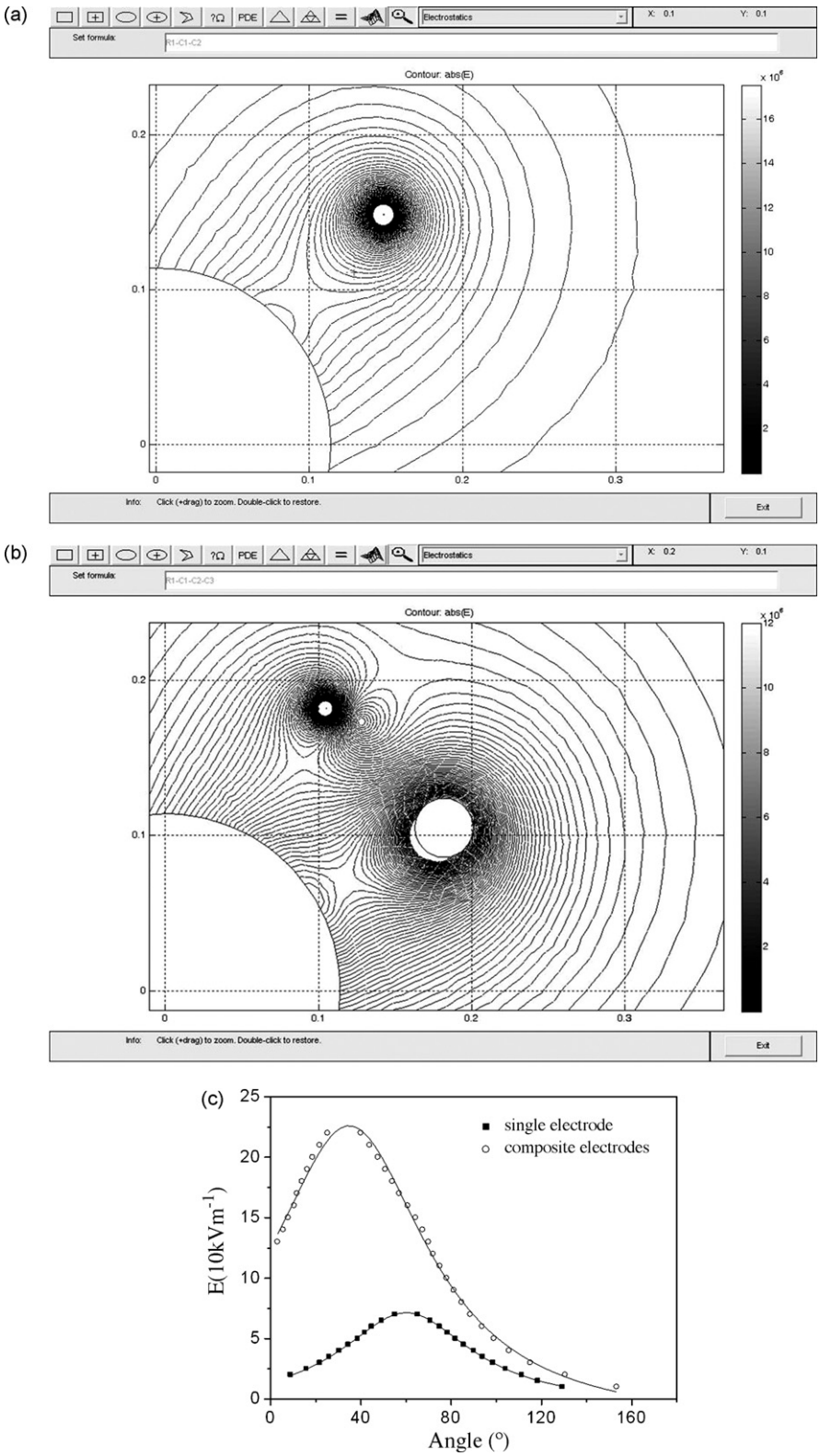

Fig. 3. Electric-field strength distributions on the rotating roll of different electrodes; (a) single electrode; (b) multi-electrodes; (c) curve of distributions. The parameters of simulation were: applied voltage $U = 20$ kV, the center distances $L = L_1 = L_2 = 0.21$ m, the radius of static electrode $R_2 = 0.019$ m, the angle of static electrode $\theta_1 = 30^\circ$, the angle of corona electrode $\theta_2 = 60^\circ$.

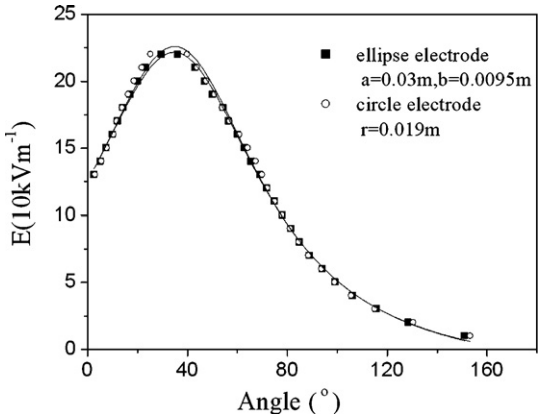

Fig. 4. Electric-field strength distributions on the rotating roll of ellipse electrode and circle electrode. The parameters of simulation were: $U = 20$ kV, $L = L_1 = L_2 = 0.21$ m, $R_2 = 0.019$ m, $\theta_1 = 30°$, $\theta_2 = 60°$.

electrode has much bigger electric strength than single electrode and the position of maximum value leans to the direction of static electrode. Because the electric field strength of static electrode was much stronger than corona electrode's, the static electrode has main influence to the distribution of electric field.

2.2. Shapes of static electrodes

The cross-section shapes of static electrodes were circle and ellipse. As shown in Fig. 4, the distributions of electric field strength were almost same when the cross sections of two shapes were close.

2.3. Applied voltages

The applied voltages were 20, 25, 30, 35 kV separately.

As shown in Fig. 5, the maximum value of the electric field strength increased with the applied voltage was increased and its position still leans to the direction of static electrode. But excessive applied voltage could lead to spark discharge which broke the process of separation.

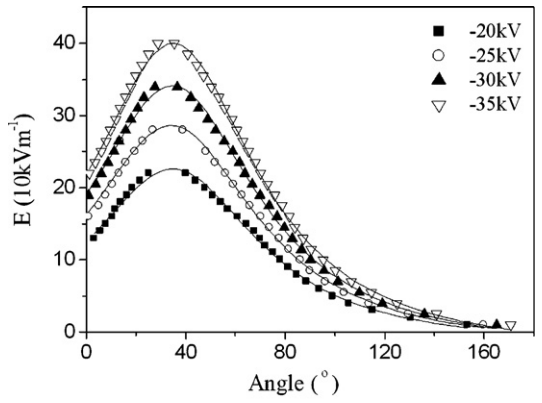

Fig. 5. Electric-field strength distributions on the rotating roll under different applied voltages. The parameters of simulation were: $L = L_1 = L_2 = 0.21$ m, $R_2 = 0.019$ m, $\theta_1 = 30°$, $\theta_2 = 60°$.

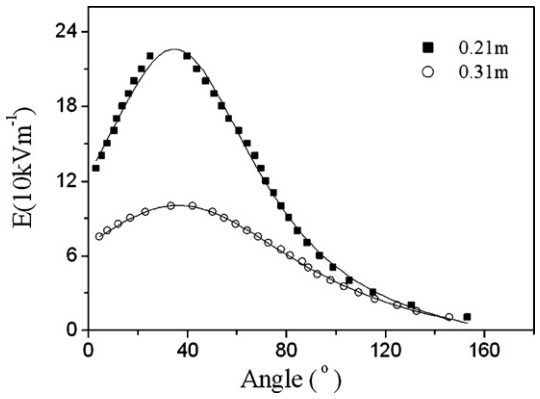

Fig. 6. Electric-field strength distributions on the rotating roll under different center distances. The parameters of simulation were: $U = 20$ kV, $R_2 = 0.019$ m, $\theta_1 = 30°$, $\theta_2 = 60°$.

2.4. Center distances

The center distances of electrode center and rotating roll center were 0.21 and 0.31 m. The center distances have a great influence to the distribution of electric field strength. As shown in Fig. 6, the distributions of electric field strength have great differences under different center distances. The maximum value of electric field strength was sharp increased when the center distance was reduced. So the small center distance was good for separation. In fact, too small center distance was not good for the separation for the spark discharge was easily created.

2.5. Sizes of static electrodes

The radiuses of static electrodes were 0.01, 0.019, 0.03 and 0.04 m separately. As shown in Fig. 7, the electric field strength increased with the radius of static electrodes increased and the total distribution of electric field was not changed. But too large static electrode could impact the corona electrode's work.

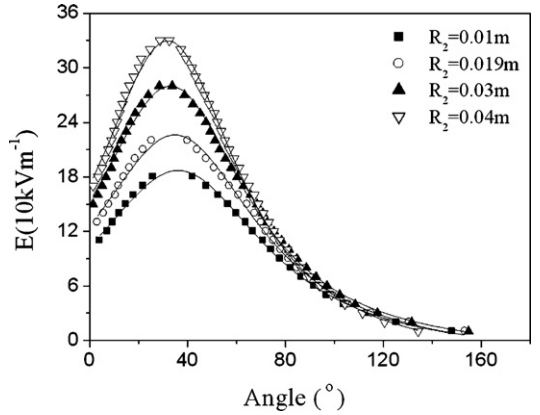

Fig. 7. Electric-field strength distributions on the rotating roll under different static electrodes radius. The parameters of simulation were: $U = 20$ kV, $L = L_1 = L_2 = 0.21$ m, $\theta_1 = 30°$, $\theta_2 = 60°$.

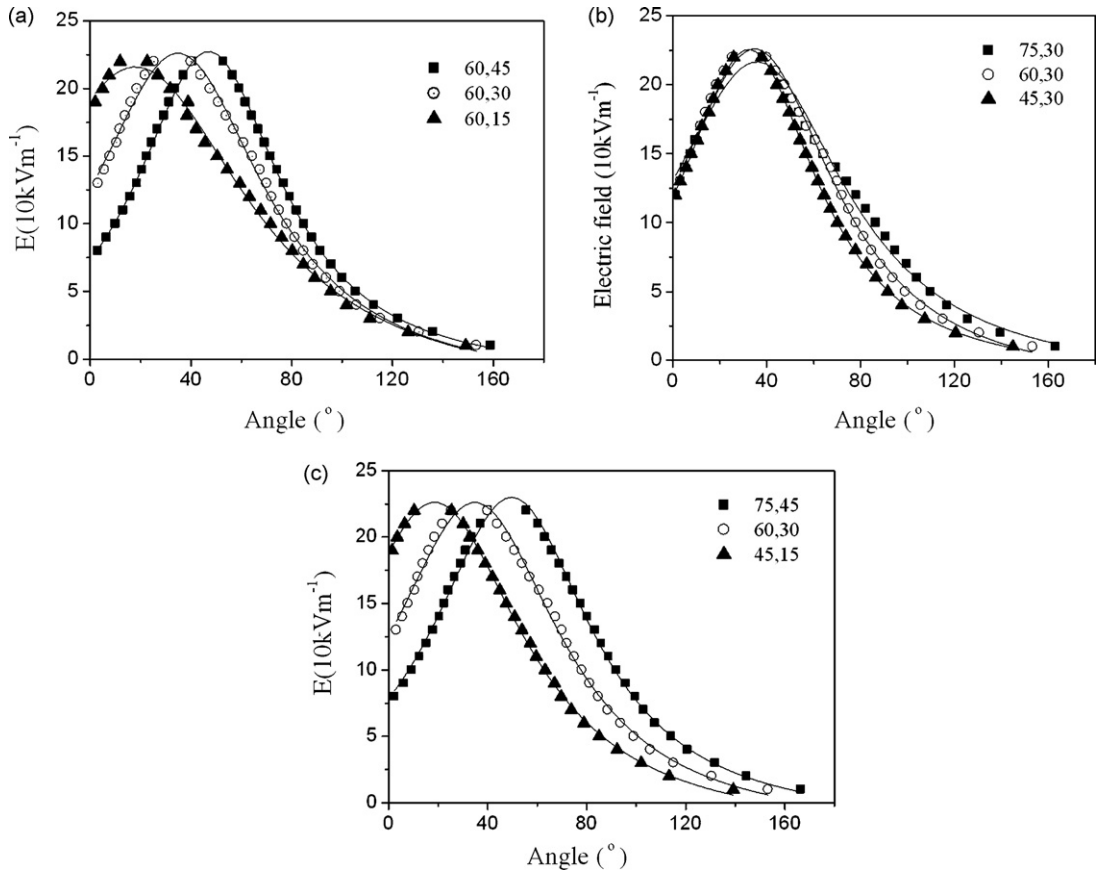

Fig. 8. Electric-field strength distributions on the rotating roll under different angles of electrodes: (a) θ_1 was changed and $\theta_2 = 60°$; (b) $\theta_1 = 30°$ and θ_2 was changed; (c) θ_1 and θ_2 were changed. The parameters of simulation were: $U = 20$ kV, $L = L_1 = L_2 = 0.21$ m, $R_2 = 0.019$ m.

2.6. Positions of electrodes

(1) The angles of θ_1 were 45°, 30° and 15° separately.
As shown in Fig. 8a, when the angle of static electrode was reduced, the maximum value of electric field strength decreased and its position followed the static electrode.
(2) The angles of θ_2 were 75°, 60° and 45° separately.
As shown in Fig. 8b, although the angle of corona electrode was changed much, the distribution of electric field strength was nearly not changed. The position of corona electrode has little influence to the distribution of electric field.
(3) The angles of θ_2 and θ_1 were (75°, 45°), (60°, 30°) and (45°, 15°) separately.
As shown in Fig. 8(c), the distribution of electric field only rotated with the angles of electrodes.

The variation of operating parameters of electrodes and applied voltages indirectly influenced the distribution of electric field, as shown above. The separating results would be improved by increasing the applied voltage and reducing the center distance. But too high applied voltage and too small center distance would lead to spark discharge which broke the process of separation. The angles of electrodes also had large influence to the distribution of electric field. From the view of charging [7], the parameter of large angle of corona electrode and low angle of static electrode is good for particles' charging. But too large angle of corona electrode lead to unsaturated charging. The optimal parameters of angles of electrodes need further study.

3. Experiments and discussion

According to the results of computer simulation, experiments were carried out toward the two major influencing factors (applied voltage and positions of electrodes). The materials used in this study were scraped waste PCBs [8].

3.1. Different applied voltages

The size of mixture particles of metals and nonmetals was −0.6 + 0.8 mm.

As shown in Fig. 9, it was found that:

(1) When $U = 15$ kV, the weight contents of five holding tanks have obvious variations and the nonmetal particles were found to adhere on the surface of rotating electrode which was the characteristic of corona discharge.
(2) The content of holding tank II sharp decreased when $U = 17.5$ kV and hold on a value about 20% from $U = 20$ kV to 30 kV. Then the applied voltage of 20 kV was good for separating nonmetal particles on the size of 0.6–0.8 mm.

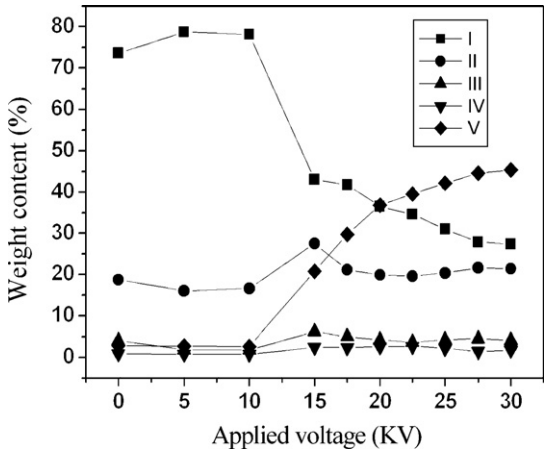

Fig. 9. weight content of particles in holding tanks under different applied voltages, I was metals, V was nonmetals, II, III and IV were middling. The operating parameters of experiment were: $L = L_1 = L_2 = 0.21$ m, $R_1 = 0.114$, $R_2 = 0.019$ m, $\theta_1 = 30^\circ$ and $\theta_2 = 60^\circ$.

(3) When $U > 15$ kV, the content of holding tank V increased with the applied voltage increased. Increasing the applied voltage increased the eliminated ratio of nonmetal particles and the purity of metal particles, which improved the separating results and had a good agreement with simulation results.

The discharge inception electric field strength of corona electrode was computed by the Peek's law:

$$E_0 = k_1(1 + k_2/r^{1/2}) \quad (1)$$

Where E_0 was the discharge inception electric field strength of corona electrode, r was the radius of corona wire. The k_1 and k_2 were related with construction of electrode, polarity of applied voltage, environmental atmosphere P and temperature T. When used parallel negative corona electrode, $T = 298$ K and $P = 101{,}325$ Pa, $k_1 = 30.1 \times 10^5$ V/m, $k_2 = 0.0301\ \mathrm{m}^{1/2}$. When $r = 0.00015$ m, the E_0 was computed to 104.074×10^5 V/m and

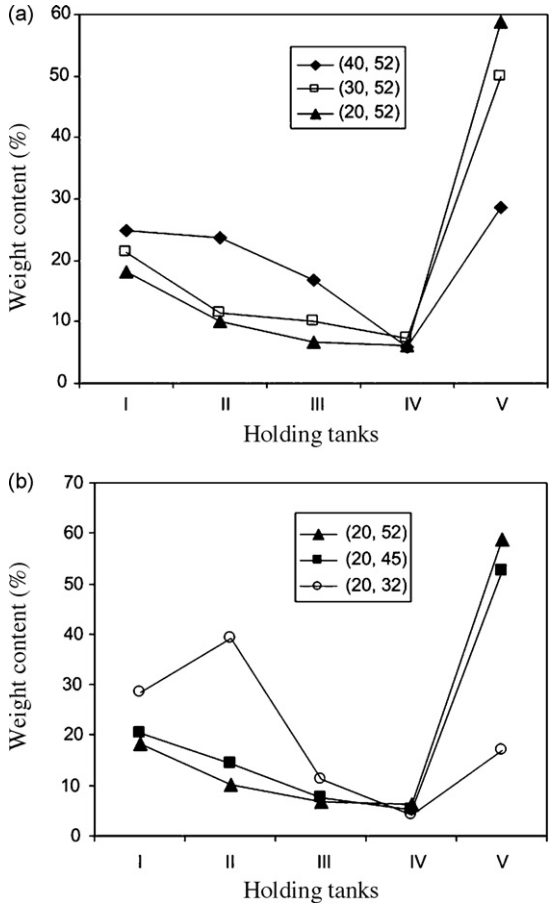

Fig. 10. Results of particles under different angle of electrodes: (a) θ_1 was changed and θ_2 was constant; (b) θ_1 was constant and θ_2 was changed. The operating parameters of experiment were: $U = 25$ kV, $L = L_1 = L_2 = 0.21$ m, $R_1 = 0.114$, $R_2 = 0.019$ m.

the discharge inception voltage was:

$$V_0 = E_0 r \ln(2L/r), \quad L \gg r \quad (2)$$

Then the V_0 was computed to 12.31 kV by the equation (2). In theoretical aspect, when the applied voltage was 12.31 kV,

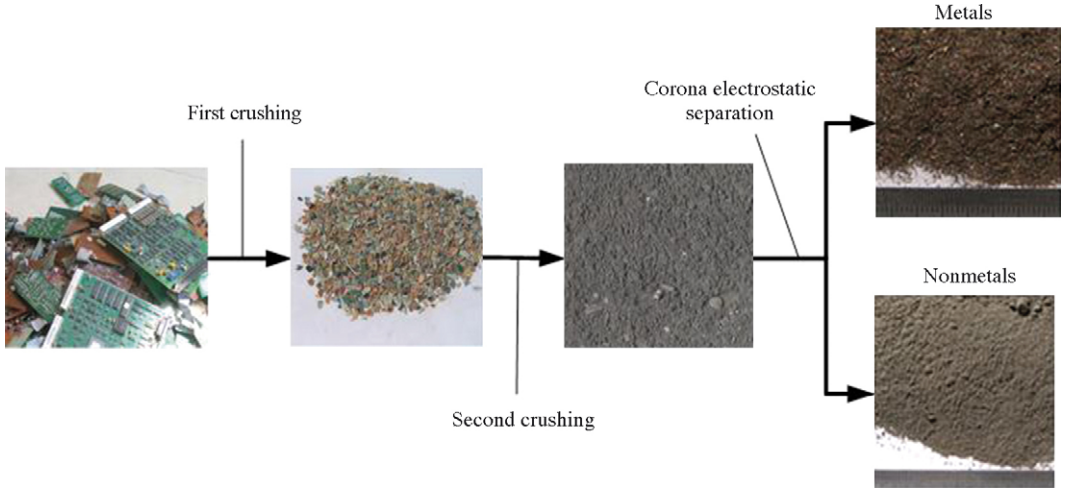

Fig. 11. Results of separating waste PCBs: $U = 20$–30 kV, $L = L_1 = L_2 = 0.21$ m, $R_1 = 0.114$, $R_2 = 0.019$ m, $\theta_1 = 20^\circ$ and $\theta_2 = 60^\circ$.

the corona discharge occur, which has a good agreement with experimental result.

3.2. Different positions of electrodes

As shown in Fig. 10(a), the contents of the middlings (II, III and IV) were reduced with the angle of static electrode decreased. As shown in Fig. 10(b), the contents of middlings were reduced with the increase of corona electrode angle. Then the large angle of corona electrode and small angle of static electrode was good for separating results, which has a good agreement with simulated results.

From the experimental results it was found that, the changes of parameters of electrodes and applied voltages influenced the distribution of electric field. The variation of distribution of electric field indirectly influenced the separating results. So the simulation of electric field could clearly and profoundly realize the process of separation and analyze the influences of operating parameters. The good separating results were shown in Fig. 11 under the optimized operating parameters.

4. Conclusions

In this paper, the computer simulation of electric field was used for optimizing the process of recycling waste PCBs by CES, it was found that: the way of increasing the applied voltage, radius of static electrode, angle of corona electrode and decreasing center distance, angle of static electrode were good for the separation. Through the correlation of simulated and experimental results, the good separation results were got under the optimized operating parameter: $U = 20$–$30\,\text{kV}$, $L = L_1 = L_2 = 0.21\,\text{m}$, $R_1 = 0.114$, $R_2 = 0.019\,\text{m}$, $\theta_1 = 20^\circ$ and $\theta_2 = 60^\circ$. The method of computer simulation was successfully used for optimizing the operating parameters of CES in recycling waste PCBs.

Acknowledgements

This project was supported by the National High Technology Research and Development Program of China (863 program 2006AA06Z364), Program for New Century Excellent Talents in University and the Research Fund for the Doctoral Program of Higher Education (20060248058).

References

[1] H.M. Veit, T.R. Diehl, et al., Utilization of magnetic and electrostatic separation in the recycling of printed circuit boards scrap, Waste Manage. 25 (2005) 67–74.
[2] Ehner Theo. Integrated recycling of non-ferrous metal at Boliden Ltd., IEEE International Symposium on Electronics & the Environment, 1998, pp. 42–47.
[3] N. Menad, Bo. Björkman, G. Eric, Allain, Combustion of plastics contained in electric and electronic scrap, Resour. Conserv. Recy. 24 (1998) 65–85.
[4] BAN (The Basel Action Network) & Silicon Valley Toxicity (SVTC, 2002): Exporting harms, http://www.svtc.org/cleancc/pubs/technotrash.
[5] A. Bernardes, I. Bohlinger, H. Milbrandt, D. Rodriguez, W. Wuth, Recycling of printed circuit boards by melting with oxidizing/reducing top blowing process, in: TMS Annual Meeting, Orlando, Flórida, EUA, 1997, pp. 363–375.
[6] Jia Li, Hongzhou Lu, Jie guo, Zhenming Xu, Yaohe Zhou, Recycle technology for recovering resources and products from waste printed circuit boards, Environ. Sci. Technol. 41 (2007) 1995–2000.
[7] M. Pauthenier, La Physique des Forces Eïlectrostatiques et Leurs Applications, C.N.R.S., Grenoble, France, 1960, pp. 279–287.
[8] Jia. Li, Zhenming Xu, Yaohe Zhou, Application of corona discharge and electrostatic force to separate metals and nonmetals from crushed particles of waste printed circuit boards, J. Electrostat. 65 (2007) 233–238.